

Measurement of Long-Range ^1H – ^1H Dipolar Couplings in Weakly Aligned Proteins

Zhengrong Wu and Ad Bax*

Laboratory of Chemical Physics, NIDDK, National Institutes of Health, Bethesda, Maryland 20892

Received May 9, 2002

Residual dipolar couplings (RDCs) can readily be measured in proteins that are weakly aligned with respect to the magnetic field, either as a result of their intrinsic magnetic susceptibility anisotropy¹ or by the use of a dilute liquid crystalline medium² or an anisotropically compressed hydrogel.^{3,4} These RDCs not only provide global structural information by aligning all bond vectors in a molecule relative to a single axis system, but they also can significantly improve local geometry⁵ and provide unique opportunities for structure validation.^{6,7} So far, mostly one-bond heteronuclear couplings and two-bond ^1H – ^{15}N and ^1H – ^{13}C interactions have been studied, which due to their short internuclear distances can yield large dipolar couplings.^{8,9} Here, we demonstrate that sensitive and accurate measurement of direct ^1H – ^1H couplings over distances of up to 7 Å is feasible. In contrast to NOE interactions, which in perdeuterated proteins also can be observed over such distances,^{10,11} dipolar couplings are not affected by spin diffusion, and their interpretation in structural terms is therefore quite straightforward.¹²

The dipolar coupling between a pair of protons, P and Q, is given by

$$D_{\text{PQ}}(\theta, \phi, r_{\text{PQ}}) = -\mu_0(h/2\pi)\gamma_{\text{H}}^2/(8\pi^2 r_{\text{PQ}}^3) A_a [(3 \cos^2 \theta - 1) + \frac{3}{2} R \sin^2 \theta \cos 2\phi] \quad (1)$$

where θ and ϕ describe the orientation of the P–Q vector relative to the molecular alignment tensor, r_{PQ} is the interproton distance, A_a is the magnitude of the alignment, and R is its rhombicity.⁹ Owing to the high ^1H magnetogyric ratio, γ_{H} , ^1H – ^1H couplings are inherently the largest. Measurement of ^1H – ^1H couplings over larger distances has remained difficult, however, because most of the dephasing of a given ^1H spin is caused by its nearest ^1H neighbors. With typically more than 25 protons within a 5-Å radius, the smaller dephasing caused by a proton outside such a sphere becomes difficult to measure. We propose two solutions to this problem: decoupling of the interactions with most of the nearest protons, and perdeuteration of the nonexchangeable protons. Deuteration has the additional advantage of decreasing the transverse relaxation rates of the remaining protons. Measurements discussed below utilized both deuteration and homonuclear decoupling, but the method is equally applicable to protonated proteins, albeit at somewhat reduced sensitivity caused by faster transverse relaxation.

The pulse sequence used (Figure 1) is of the quantitative J correlation type^{12,13} and measures the fraction of magnetization transferred from one proton to another (cross-peak) relative to the untransferred magnetization (diagonal). The approach is demonstrated for H^{N} – H^{N} but is easily converted to other interactions. The pulse scheme concatenates two semiselective HMQC experiments^{12,14} and is referred to as SS-HMQC2. ^1H – ^1H dephasing takes place between time points a and d, whereas for most of this time

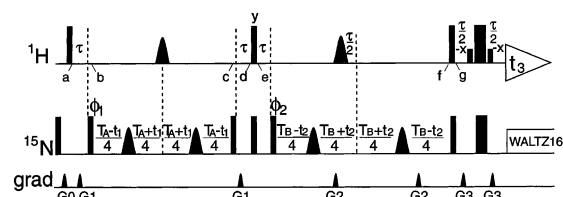


Figure 1. Pulse scheme of the 3D SS-HMQC2 experiment. Narrow and wide pulses correspond to flip angles of 90° and 180° , respectively. Low amplitude corresponds to selective (1 ms) 90° H_2O pulses. All pulses are along x , unless specified otherwise. The four shaped ^{15}N 180° pulses are of the hyperbolic secant adiabatic inversion type with durations of 1 ms each; shaped ^1H pulses are 180° reBURP.²⁰ ^{13}C decoupling (not shown) is used for samples that include ^{13}C enrichment. Prior to time point g, the ^1H carrier is at 8 ppm; after g it is switched to H_2O . Delay durations: $\tau = 5.3$ ms; T_A and T_B are typically in the 30–80 ms range. Phase cycling: $\phi_1 = x, -x$; $\phi_2 = 2x, 2(-x)$; receiver = $x, -x, -x, x$. Quadrature in both ^{15}N dimensions is obtained by altering ϕ_1 and ϕ_2 , respectively, in the regular States–TPPI manner. Pulsed field gradients are sine-bell shaped with durations of $G_{0,1,2,3} = 1, 1, 0.5, 0.5$ ms, with peak amplitudes of 25 G/cm, and directions $G_{0,1,2,3} = (xy), x, y, z$.

(between b and c) the signal exists as ^1H – ^{15}N multiple quantum coherence (MQC). Transverse relaxation of this MQC contains no $J(0)$ ^1H – ^{15}N dipolar terms, thereby enhancing sensitivity, and signals are encoded by the ^{15}N chemical shift between time points b and c. The reBURP pulse applied at the midpoint between a and d affects only the amide protons and therefore rephases all $J_{\text{HN}\alpha}$ and dipolar interactions between amide and aliphatic protons but leaves H^{N} – H^{N} dephasing intact. So, initial magnetization H^1_y (time point a) evolves to yield

$$\begin{aligned} \text{H}^1_y \rightarrow & -2 \cos(\Omega_{\text{N}^1} t_1) \sin(\pi D_{\text{H}^1\text{H}^2} T_A) \prod_{j \neq 2} \cos(\pi D_{\text{H}^1\text{H}^j} T_A) \text{H}^1_x \text{H}^2_z \\ & + \cos(\Omega_{\text{N}^1} t_1) \prod_j \cos(\pi D_{\text{H}^1\text{H}^j} T_A) \text{H}^1_y + \text{other terms} \quad (2) \end{aligned}$$

just prior to the 90°_y (^1H) COSY-type mixing pulse (time point d). This 90°_y pulse converts $\text{H}^1_x \text{H}^2_z$ into $\text{H}^1_z \text{H}^2_x$ and leaves the H^1_y term unaffected. A subsequent second HMQC element (between e and f) partially rephases the $\text{H}^1_z \text{H}^2_x$ term and dephases H^1_y , the amplitudes of which are t_2 -modulated by the ^{15}N frequency (Ω_{N^2} and Ω_{N^1} , respectively). Only the $\text{H}^2_x \text{N}^2_z$ (yielding the H^1 – H^2 cross-peak) and $\text{H}^1_x \text{N}^1_z$ (H^1 diagonal) terms, remaining after the subsequent 90°_x ^1H pulse (time point g), are converted into observable ^1H signal during the subsequent WATERGATE ^1H – $\{^{15}\text{N}\}$ rephasing period. If for protons P and Q the $\text{P} \rightarrow \text{Q}$ and $\text{Q} \rightarrow \text{P}$ cross-peak intensities are I_{PQ} and I_{QP} , their product divided by their respective diagonals is given by

$$I_{\text{PQ}} I_{\text{QP}} / I_{\text{PP}} I_{\text{QQ}} = \tan^2(\pi D_{\text{PQ}} T_A) \tan^2(\pi D_{\text{PQ}} T_B) \quad (3)$$

Equation 3 ignores fractional labeling of the amides, and a correction must be applied if incomplete protonation of amides is

* Corresponding author. E-mail: bax@nih.gov.

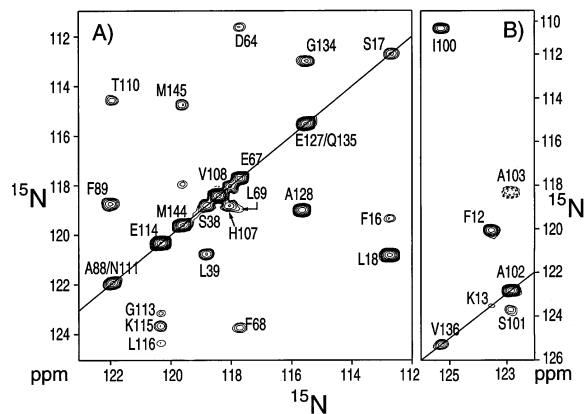


Figure 2. Two cross sections through the 600-MHz 3D SS-HMQC2 spectrum of 1.0 mM $^{15}\text{N}/^{13}\text{C}/^2\text{H}$ Ca^{2+} -calmodulin, pH 6.8, 10 mM CaCl_2 , in 95% $\text{H}_2\text{O}/5\%$ D_2O , 16 mg/mL Pf1, using $T_A = T_B = 50$ ms. (A) Taken at $F_3 = 8.15$ ppm; (B) $F_3 = 9.38$ ppm. Data were acquired as $38^* \times 36^* \times 512^*$ data matrixes, corresponding to $t_{1,\text{max}} = 38$ ms, $t_{2,\text{max}} = 36$ ms, and $t_{3,\text{max}} = 63.9$ ms. Dashed contours correspond to negative intensity.

significant (Supporting Information). Otherwise, use of eq 3 is insensitive to the amounts of initial magnetization for protons P and Q, incomplete T_1 relaxation between scans, and values of the passive couplings ($\prod_{j \neq 2}$ term in eq 2). If for all couplings to a given amide $D_{\text{HH}} \ll 1/(2T)$, and initial magnetizations of P and Q are similar, an approximate value for D_{PQ} derived from $I_{\text{cross}}/I_{\text{diag}} \approx \tan(\pi D_{\text{PQ}} T_A) \tan(\pi D_{\text{PQ}} T_B)$ may suffice. Although less accurate, this approximation can be useful if one of the diagonal or cross-peak intensities cannot be measured accurately due to overlap.

Figure 2 shows two cross sections from the 3D spectrum of Ca^{2+} -calmodulin in liquid crystalline Pf1 medium.¹⁵ Diagonals correspond to protons resonating at $F_3 = 8.15$ (Figure 2A) and 9.38 ppm (Figure 2B); cross-peaks are seen to F_1 ^{15}N frequencies of amides dipolar coupled to the F_3 protons, which are dispersed along F_2 by their own ^{15}N shift. Most interactions in this highly α -helical protein correspond to short (~ 2.8 Å) sequential $\text{H}^{\text{N}}-\text{H}^{\text{N}}$ couplings. Although the sequential $\text{H}^{\text{N}}-\text{H}^{\text{N}}$ distances in α -helices are rather uniform, the orientations of $\text{H}^{\text{N}}-\text{H}^{\text{N}}$ vectors in a helix differ strongly from one another, resulting in very different couplings. Numerous nonhelical interactions (e.g., V136- H^{N} to I100- H^{N} in Figure 2B) also give rise to observable cross-peaks. The distance cutoff for observation of cross-peaks in the SS-HMQC2 calmodulin spectrum is over 6 Å for interproton vectors nearly parallel to the alignment tensor z axis (e.g., E114- H^{N} to L116- H^{N}).

To evaluate the intrinsic accuracy of the method, we also measured D_{HH} values in the protein ubiquitin. Comparison of D_{HH} with ubiquitin's solution structure⁶ shows excellent agreement (Figure 3), with a Pearson's correlation coefficient $R_p = 0.985$, and only slightly lower agreement, $R_p = 0.95$, with its crystal structure.¹⁶ Distances exceeding 7 Å are observed in this protein (Supporting Information). D^{calc} values in Figure 3 were calculated using an alignment tensor derived from $^{15}\text{N}-^1\text{H}$ dipolar couplings (using a librationaly corrected 1.04 Å r_{NH} value). The slope of the correlation is very close to unity, indicating that internal dynamics has comparable effects on $^1\text{H}-^1\text{H}$ and one-bond $^1\text{H}-^{15}\text{N}$ interactions.

The SS-HMQC2 method presented here for measurement of $^1\text{H}^{\text{N}}-^1\text{H}^{\text{N}}$ dipolar couplings relies on selective removal of a large fraction of coupling partners by either selective (de)coupling, deuteration, or both. This approach can readily be adapted to study different types of interactions (e.g., $\text{H}^{\alpha}-\text{H}^{\alpha}$ in proteins or base-base and $\text{H}1'-\text{H}1'$ in nucleic acids).

Quantitative J -correlation does not yield the sign of the dipolar coupling. Analogous to other schemes,^{17,18} the pulse scheme of

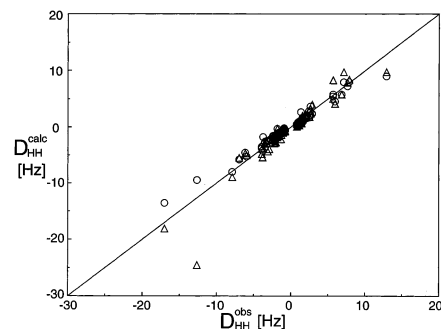


Figure 3. Comparison of 86 D_{HH} dipolar couplings, measured for ubiquitin in the presence of a 5% w/w dodecyl-PC/dihexyl-PC/CTAB bicelle mixture (molar ratio of 33:10:1.5), with values $D_{\text{HH}}^{\text{calc}}$ predicted on the basis of (O) the NMR structure (PDB entry 1D3Z⁶) and (Δ) the X-ray structure (PDB entry 1UBI¹⁶). The predicted couplings were calculated for an alignment tensor with $D_a^{\text{NH}} = 11.9$ Hz, $R = 0.40$. The sign of the observed coupling is selected in accordance with the calculated value.

Figure 1 can be adapted to yield such sign information by insertion of a spin-state selection filter prior to t_1 evolution, using a small flip angle at time point d and removal of the purge pulse at time point f. However, this approach lowers the signal-to-noise ratio and therefore is not applicable to some of the smallest D_{HH} couplings measured here. In our experience, structure calculation based on the absolute D_{HH} value¹⁹ is adequate. It works particularly well when sufficient other structural parameters are available, where use of absolute D_{HH} values does not cause serious convergence problems. In contrast to one-bond heteronuclear couplings,⁵ the internuclear distance is a variable when using D_{HH} in structure calculations.¹⁹

The possibility to observe direct dipolar interactions in weakly aligned macromolecules over longer distances offers new opportunities in the study of protein structure and dynamics.

Acknowledgment. We thank S. Grzesiek and S. P. Li for the samples of $^2\text{H}/^{13}\text{C}/^{15}\text{N}$ ubiquitin and calmodulin.

Supporting Information Available: Equation 3, adapted for incomplete protonation; one figure illustrating >7 Å direct dipolar connectivities in ubiquitin (PDF). This material is available free of charge via the Internet at <http://pubs.acs.org>.

References

- (1) Tolman, J. R.; Flanagan, J. M.; Kennedy, M. A.; Prestegard, J. H. *Proc. Natl. Acad. Sci. U.S.A.* **1995**, *92*, 9279.
- (2) Tjandra, N.; Bax, A. *Science* **1997**, *278*, 1111.
- (3) Tycko, R.; Blanco, F. J.; Ishii, Y. *J. Am. Chem. Soc.* **2000**, *122*, 9340.
- (4) Sass, H. J.; Musco, G.; Stahl, S. J.; Wingfield, P. T.; Grzesiek, S. *J. Biomol. NMR* **2000**, *18*, 303.
- (5) Tjandra, N.; Omichinski, J. G.; Gronenborn, A. M.; Clore, G. M.; Bax, A. *Nat. Struct. Biol.* **1997**, *4*, 732.
- (6) Cornilescu, G.; Marquardt, J. L.; Ottiger, M.; Bax, A. *J. Am. Chem. Soc.* **1998**, *120*, 6836.
- (7) Clore, G. M.; Garrett, D. S. *J. Am. Chem. Soc.* **1999**, *121*, 9008.
- (8) Yang, D. W.; Venters, R. A.; Mueller, G. A.; Choy, W. Y.; Kay, L. E. *J. Biomol. NMR* **1999**, *14*, 333.
- (9) Bax, A.; Kontaxis, G.; Tjandra, N. *Methods Enzymol.* **2001**, *339*, 127.
- (10) Venters, R. A.; Metzler, W. J.; Spicer, L. D.; Mueller, L.; Farmer, B. T. *J. Am. Chem. Soc.* **1995**, *117*, 9592.
- (11) Mal, T. K.; Matthews, S. J.; Kovacs, H.; Campbell, I. D.; Boyd, J. J. *J. Biomol. NMR* **1998**, *12*, 259.
- (12) Tian, F.; Fowler, C. A.; Zartler, E. R.; Jenney, F. A.; Adams, M. W.; Prestegard, J. H. *J. Biomol. NMR* **2000**, *18*, 23.
- (13) Bax, A.; Vuister, G. W.; Grzesiek, S.; Delaglio, F.; Wang, A. C.; Tschudin, R.; Zhu, G. *Methods Enzymol.* **1994**, *239*, 79.
- (14) Bax, A.; Griffey, R. H.; Hawkins, B. *J. Magn. Reson.* **1983**, *55*, 301.
- (15) Hansen, M. R.; Mueller, L.; Pardi, A. *Nat. Struct. Biol.* **1998**, *5*, 1065.
- (16) Vijay-Kumar, S.; Bugg, C. E.; Cook, W. J. *J. Mol. Biol.* **1987**, *194*, 531.
- (17) Ottiger, G.; Ruckert, M.; Levitt, M. H.; Moshref, A. *J. Biomol. NMR* **2000**, *16*, 343.
- (18) Peti, W.; Griesinger, C. *J. Am. Chem. Soc.* **2000**, *122*, 3975.
- (19) Tjandra, N.; Marquardt, J.; Clore, M. *J. Magn. Reson.* **2000**, *142*, 393.
- (20) Geen, H.; Freeman, R. *J. Magn. Reson.* **1991**, *93*, 93.

JA026845N